

# Cryogenic Temperature Effects on Guided Wave Structural Health Monitoring Signals in Unidirectional Carbon Fiber Reinforced Plastics

---

SHANKAR GALIANA<sup>1,2,\*</sup>, BHOOSHIT PATEL<sup>2</sup>,  
MARIA MOIX-BONET<sup>1,2</sup>, DANIEL SCHMIDT<sup>1</sup>  
and PETER WIERACH<sup>1,2</sup>

## ABSTRACT

Structural Health Monitoring (SHM) is a promising technology for enhancing the safety and performance of high-value composite structures operating in extreme environments, such as cryogenic temperatures encountered in aerospace systems, hydrogen storage tanks, and emerging space applications. These structures are subject to significant mechanical and thermal stresses that can degrade material properties, increase brittleness, and threaten structural integrity. In such conditions, traditional inspection methods may be infeasible or insufficient, while SHM enables real-time, in-situ damage detection and continuous monitoring throughout a structure's service life. Among SHM techniques, Guided Wave (GW) methods offer significant advantages for fiber-reinforced polymer composites due to their long-range propagation capability and sensitivity to various defect types, including delaminations, matrix cracking, and impact damage. However, GW signals are also influenced by environmental and operational factors such as temperature variations, mechanical loading, and adjacent media (e.g., moisture, frost, or liquid interfaces), which can complicate signal interpretation and potentially mask real damages or produce false positives.

This study investigates the effects of cryogenic temperature and surrounding media on GW signal behavior in a unidirectional carbon fiber-reinforced polymer panel equipped with co-bonded DuraAct™ piezoceramic transducers. The specimen is exposed to controlled thermal cycling, including immersion in liquid nitrogen, and guided wave responses are measured across a wide frequency range.

Results reveal distinct frequency and temperature-dependent behavior in both S<sub>0</sub> and A<sub>0</sub> wave modes. Observed changes in amplitude and time-of-flight are linked to transducer performance, material stiffening, and boundary media interactions. These findings highlight the critical need for environmental compensation in guided wave SHM systems and highlight opportunities to monitor both structural health and environmental conditions using wave behavior in applications spanning aeronautics, hydrogen energy systems, and space technologies.

---

<sup>1</sup>Institute of Lightweight Systems, German-Aerospace-Center (DLR) Lilienthalplatz 7, 38108 Braunschweig, Germany

<sup>2</sup>Institut für Polymerwerkstoffe und Kunststofftechnik, TU Clausthal Adolph-Roemer-Straße 2A, 38678 Clausthal-Zellerfeld, Germany

## 1. INTRODUCTION

Structural Health Monitoring (SHM) is a promising technology for improving the safety and reliability of critical structures, especially those exposed to extreme environments where conventional inspection is impractical or inaccessible. Applications such as aerospace systems and hydrogen tanks often face thermal and mechanical loads that can degrade material properties and compromise structural integrity [1, 2]. SHM enables autonomous, in-situ damage detection and continuous monitoring throughout the service life of such components [3, 4].

Carbon fiber-reinforced polymers (CFRPs), widely used in aerospace and cryogenic systems, offer excellent strength-to-weight ratios and corrosion resistance [1, 5]. However, they remain vulnerable to delamination, matrix cracking, and thermal fatigue, particularly under cryogenic cycling, where increased stiffness and brittleness exacerbate damage progression [5–7].

Among SHM methods, guided wave (GW) techniques are especially well-suited for CFRPs, offering large-area coverage, high defect sensitivity, and low power requirements [3, 4, 8]. These systems typically use piezoelectric transducers to transmit and receive ultrasonic waves sensitive to internal damage [4, 9]. Their relevance is growing in civil aviation, hydrogen infrastructure, and lightweight aerospace applications.

However, GW-SHM performance can be strongly influenced by environmental conditions. Factors such as temperature fluctuations, frost, or liquid hydrogen exposure may alter wave propagation and sensor response, potentially masking real damage or producing false positives [8–11]. Cryogenic conditions are particularly challenging, as both CFRP properties and piezoelectric transducer performance degrade significantly at low temperatures [7, 11–13].

This study builds on prior work using DuraAct™ transducers on quasi-isotropic laminates [14] and extends it to a unidirectional (UD) CFRP panel to assess directional effects. Guided wave signals are recorded during controlled thermal cycles involving liquid nitrogen (LN<sub>2</sub>) immersion and natural convection heating. Signal features such as amplitude and time-of-flight (ToF) shifts are analyzed to evaluate the effects of cryogenic exposure on wave behavior and sensor performance.

The findings support the development of reliable GW-SHM systems for cryogenic hydrogen storage and advanced aerospace structures, contributing to improved safety, maintenance, and integration of SHM into next-generation cryogenic technologies.

## 2. MATERIALS AND METHODS

### 2.1. Specimen Configuration

The test specimen used in this study, illustrated in Figure 1 (a), consists of a UD-CFRP panel instrumented with co-bonded DuraAct™ transducers to evaluate guided wave SHM performance at cryogenic temperatures. The DuraAct™ transducer, developed by PI Ceramic GmbH, is a commercial piezocomposite acousto-ultrasonic sensor. It incorporates a soft PZT piezoceramic material (PIC255), sandwiched between metallized electrodes and encapsulated within a polyester fleece-reinforced laminate, providing both electrical insulation and mechanical flexibility. Electrical connection is achieved via two solder pads located at one end of the transducer.

The CFRP laminate of 700 mm × 500 mm was manufactured using HexPly® 8552-IM7 unidirectional prepreg, with a  $[0]_{18}$  stacking sequence. Each ply has a nominal thickness of 0.125 mm. A total of eleven DuraAct™ transducers were co-bonded onto the panel surface, arranged to enable signal transmission and reception in three primary directions: longitudinal ( $0^\circ$ , along the fiber), transverse ( $90^\circ$ , across the fiber), and diagonal ( $\pm 45^\circ$ ). Each guided wave propagation path includes one actuator and two sensors, spaced at 157 mm and 222 mm intervals, as illustrated in Figure 1 (b). Following transducer integration, the entire assembly was autoclave-cured, yielding a consolidated laminate thickness of approximately 2.25 mm.

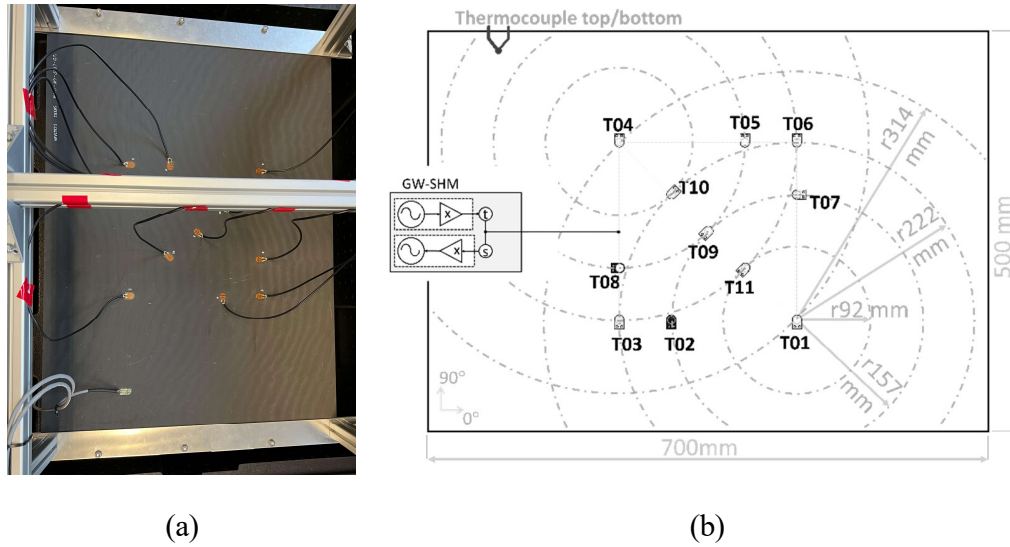


Figure 1: (a) UD-CFRP panel instrumented with DuraAct™ transducers and thermocouples and (b) schematic of the transducer network and propagation paths.

## 2.2. Thermal Test Set-Up

The CFRP panel is mounted using aluminum clamps positioned along its  $90^\circ$  (transverse) axis and secured to a vertically movable lifting mechanism. This system enables precise and repeatable immersion of the specimen into a  $\text{LN}_2$  bath while maintaining the panel in a vertical orientation, perpendicular to the cryogenic liquid surface during both immersion and withdrawal.

The integrated transducer network is interfaced with a PXIe-based guided wave SHM acquisition system supplied by National Instruments. Two thermocouples are bonded to the top and bottom surfaces of the panel to monitor temperature variations during testing. The complete experimental configuration is depicted in Figure 2 (a).

During each thermal cycle, the panel is fully submerged in the  $\text{LN}_2$  bath until thermal equilibrium is reached, typically at approximately  $-197^\circ\text{C}$ . It is then gradually lifted and allowed to warm to ambient room temperature ( $\sim 15^\circ\text{C}$ ) through natural convection in air. Throughout this process, guided wave signals are continuously recorded. Excitation frequencies range from 20 kHz to 250 kHz in 10 kHz increments, providing broadband signal characterization across the thermal gradient. A representative temperature profile, captured by the top-surface thermocouple, is shown in Figure 2 (b).

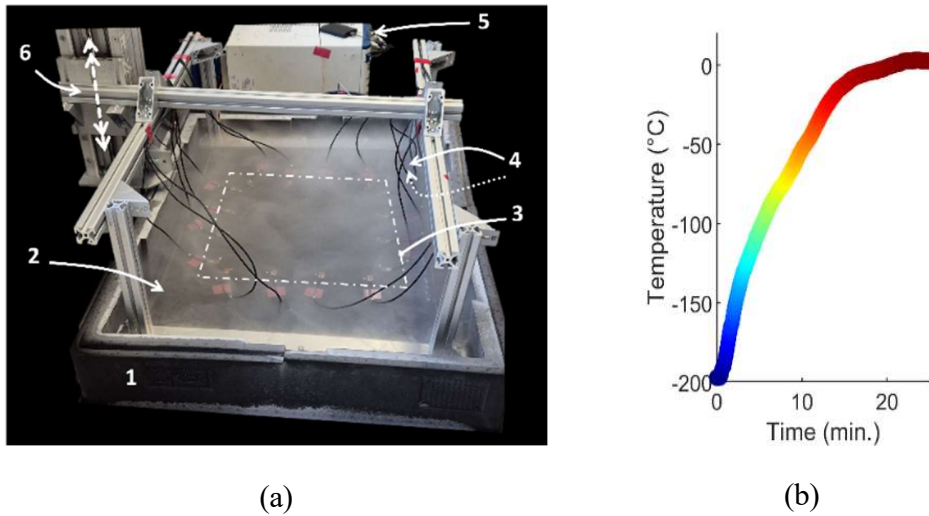


Figure 2: (a) Experimental setup showing: (1) cryogenic bath, (2) UD-CFRP panel, (3) transducer network, (4) thermocouples, (5) data acquisition system, and (6) lifting mechanism, and (b) representative temperature profile from the top-surface thermocouple during thermal cycling.

### 3. RESULTS AND DISCUSSIONS

#### 3.1. Guided Wave Signal Temperature Response

In this study, guided wave excitation was carried out using transducer 4 (T4), which generated a five-cycle Hanning-windowed sine burst with a peak amplitude of 50 V. Waveforms were acquired along the  $0^\circ$  (fiber) direction using transducer 5 (T5) and along the  $90^\circ$  (transverse) direction using transducer 8 (T8), allowing for the analysis of anisotropic wave behavior in the UD-CFRP laminate. The recorded signals were processed through a multi-step pipeline including denoising, cross-talk removal, Hilbert transform-based envelope extraction, and peak detection for each estimated propagating mode.

Maximum signal amplitudes and ToF values were extracted for both A0 and S0 mode approximations across a frequency sweep from 20 kHz to 250 kHz in 10 kHz increments. These parameters were used to evaluate dispersion characteristics and temperature sensitivity under cryogenic and ambient conditions.

The A0 mode remained clearly identifiable up to 150 kHz in the fiber direction and 70 kHz in the transverse direction. Above these frequencies, signal quality deteriorated due to attenuation, mode overlap and interference. Conversely, the S0 mode only became distinguishable above 120 kHz, as lower-frequency signals produced amplitudes too weak for consistent detection.

Figure 3 (a) presents the maximum amplitude response of the A0 mode across the frequency spectrum for both the fiber ( $0^\circ$ ) and transverse ( $90^\circ$ ) directions. Two distinct trends are observed. Along the fiber direction, signal amplitudes are approximately an order of magnitude higher than those recorded in the transverse direction, demonstrating the influence of directional stiffness and waveguiding in the unidirectional laminate.

In the  $0^\circ$  direction, low-frequency A0 amplitudes exhibit a near-constant plateau as the temperature decreases from room temperature to around  $-65^\circ\text{C}$ . Below this temperature, amplitudes progressively decline in a near-linear trend down to  $-197^\circ\text{C}$ .

In contrast, higher frequencies show an initial logarithmic increase in amplitude as the temperature drops from room temperature to  $-65\text{ }^{\circ}\text{C}$ , followed by a similar linear decay toward  $-197\text{ }^{\circ}\text{C}$ . The peak amplitude along the fiber direction occurs near 90 kHz.

In the transverse direction ( $90^{\circ}$ ), a different trend is observed. Across the entire frequency range, amplitudes decrease monotonically with decreasing temperature, without a plateau or initial rise. The maximum amplitude in this direction occurs near 40 kHz, significantly lower than in the fiber direction.

Figure 3 (b) shows the corresponding amplitude response for the S0 mode. Both directions exhibit a clear monotonic decrease in amplitude with decreasing temperature. However, the amplitudes measured along the fiber direction remain equal at low frequencies but up to ten times higher than in the transverse direction at higher frequencies. The frequency at which maximum amplitude occurs in the fiber direction is also shifted about 100 kHz higher compared to the transverse orientation.

Figure 4 (a) illustrates the ToF of the A0 mode across the frequency spectrum for both directions. A clear difference is observed, with ToF values consistently higher in the transverse direction, indicating lower phase velocities relative to the fiber direction. This reflects the material's anisotropy, where wave propagation is faster along the stiffer fiber axis.

As temperature decreases, ToF values show a monotonic reduction in both directions. However, the reduction is much more pronounced in the transverse direction, suggesting a considerable increase in phase velocity likely due to the stiffening of the polymer matrix. Along the fiber direction, ToF reductions are relatively small, implying that the axial stiffness, dominated by the carbon fibers, is less affected by temperature.

Figure 4 (b) shows the ToF behavior for the S0 mode across the same frequency range. The trends are qualitatively similar to those observed in the A0 mode. The transverse direction consistently shows higher ToF values than the fiber direction, and ToF reduction with temperature is more significant in the transverse direction. This further supports the idea that matrix properties, more influential in the transverse direction, undergo greater stiffening at cryogenic temperatures, increasing phase velocity.

When comparing ToF and amplitude spectra, different patterns emerge. ToF appears strongly correlated with CFRP stiffness, particularly with the matrix-dominated transverse direction. In contrast, amplitude behavior seems influenced by additional factors. While attenuation and viscoelastic damping contribute, especially transversely, they do not fully explain the amplitude decrease at low temperatures.

A more plausible explanation involves changes in transducer behavior. The reduction in piezoelectric efficiency at cryogenic temperatures, along with increased precompression of the DuraAct™ transducers, may explain the reduced amplitudes in both A0 and S0 modes.

One open point is the increase in A0 amplitude along the fiber direction down to  $-65\text{ }^{\circ}\text{C}$ . If caused by reduced matrix damping, a stronger effect might be expected in the transverse direction. However, the data do not support this. An alternative explanation may be that flexural stiffness increases along the fiber direction as the matrix stiffens, improving A0 propagation, while this effect may not be as significant in the transverse direction, where flexural rigidity remains low for the lack of continuous fiber reinforcement.

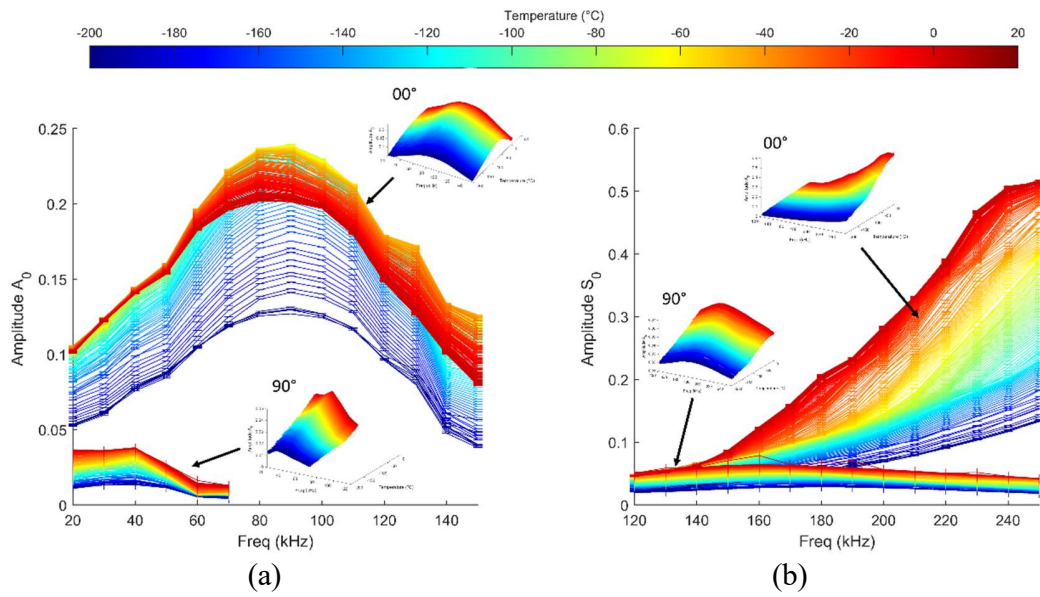


Figure 3: Maximum amplitude spectra as a function of temperature for  $0^\circ$  and  $90^\circ$  directions for (a) A0 mode and (b) S0 mode.

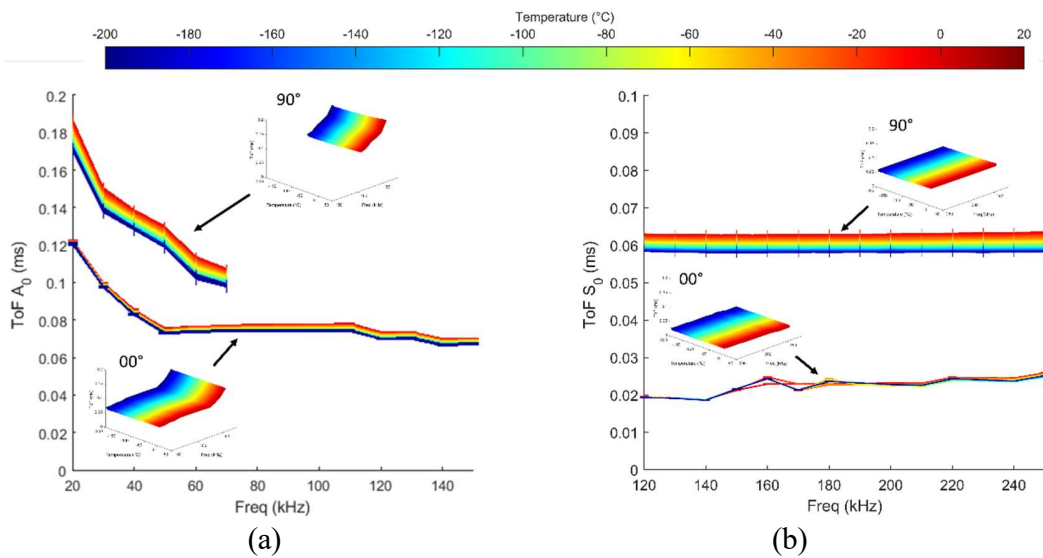


Figure 4: Time-of-flight (ToF) spectra as a function of temperature for  $0^\circ$  and  $90^\circ$  directions for (a) A0 mode and (b) S0 mode.

### 3.2. Guide Wave Adjacent Media Response

In addition to temperature effects, this study examined the influence of surrounding media, specifically LN<sub>2</sub> and gaseous nitrogen (GN<sub>2</sub>), on guided wave behavior. These conditions reflect real-world cryogenic environments in applications such as hydrogen storage tanks, where composite structures can be partially or fully in contact with cryogenic liquids and vapors.

Three configurations were tested using the same UD-CFRP specimen:

- Fully Immersed: Both top (with transducers) and bottom surfaces submerged in LN<sub>2</sub> at  $-197\text{ }^{\circ}\text{C}$ .
- Partially Immersed: Bottom in LN<sub>2</sub> at  $-197\text{ }^{\circ}\text{C}$ , top exposed to GN<sub>2</sub> at  $-193\text{ }^{\circ}\text{C}$ .
- Fully Emerged: Entire panel in GN<sub>2</sub>, with bottom at  $-195\text{ }^{\circ}\text{C}$  and top at  $-183\text{ }^{\circ}\text{C}$ .

Figure 5 presents the guided wave responses for these conditions, with amplitude and ToF values linearly compensated to normalize the top surface temperature to a reference of  $-197\text{ }^{\circ}\text{C}$ .

For the S<sub>0</sub> mode, both maximum amplitude and ToF remained nearly unchanged across all configurations, indicating minimal sensitivity to adjacent media. This confirms the S<sub>0</sub> mode's robustness, due to its in-plane motion and limited interaction with external boundaries.

In contrast, the A<sub>0</sub> mode showed clear sensitivity to full immersion. Both amplitude and ToF changed significantly between the fully immersed and emerged states. Immersion likely introduces mechanical constraint and energy loss to the LN<sub>2</sub>, while GN<sub>2</sub> offers reduced mechanical constraint, enabling better transducer coupling and signal transmission.

The similarity between partially immersed and fully emerged conditions suggests the formation of a gaseous insulation layer (film boiling) on the submerged surface during testing, effectively making both cases behave as fully emerged.

In summary, the S<sub>0</sub> mode is resilient to media effects, while the A<sub>0</sub> mode responds to mechanical and thermal boundary conditions. This distinction is critical for accurate GW-SHM in cryogenic tanks, where variable fill levels and media interfaces may affect signal interpretation.

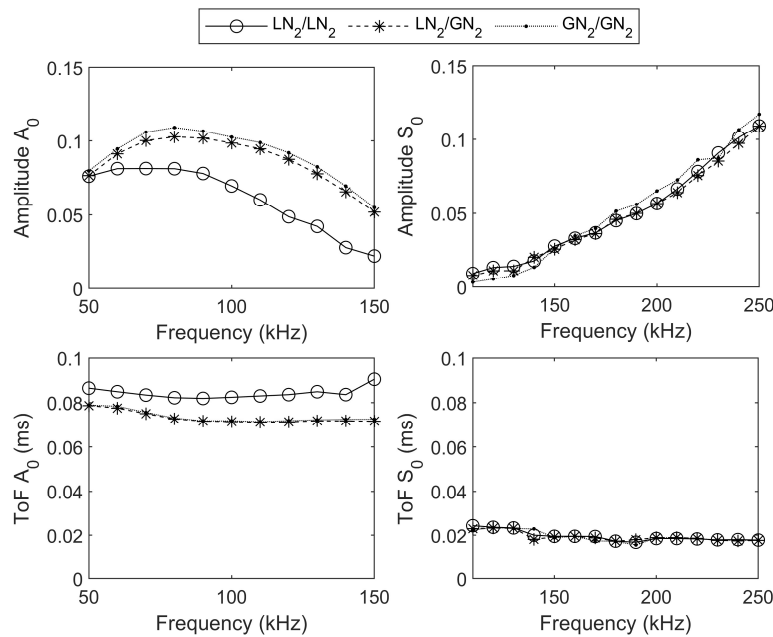


**Figure 5:** Comparison of linearly compensated amplitude and time-of-flight (ToF) spectra for A<sub>0</sub> and S<sub>0</sub> modes across different immersion conditions.

#### 4. CONCLUSIONS

This study investigated the behavior of guided wave signals in a UD-CFRP panel equipped with co-bonded DuraAct™ piezocomposite transducers under cryogenic

conditions. By subjecting the specimen to controlled thermal cycling, including immersion in liquid nitrogen, and evaluating the guided wave responses across a broad frequency range, key insights were gained into the influence of temperature and adjacent media on SHM system performance.

The results demonstrate strong anisotropic behavior in both amplitude and ToF responses, particularly between fiber-aligned and transverse wave propagation paths. ToF trends were closely linked to temperature-induced stiffening of the CFRP matrix, especially in directions dominated by matrix properties. In contrast, amplitude variations were less clearly attributed to material changes and more likely influenced by transducer performance degradation at low temperatures.

Adjacent media, specifically the difference between liquid and gaseous nitrogen, had a pronounced effect on the A0 mode, impacting both amplitude and ToF. The S0 mode, however, remained largely insensitive to boundary conditions, underlining its potential as a robust channel for SHM in variable cryogenic environments.

These findings underscore the importance of considering both material anisotropy and environmental boundary effects in the design and calibration of guided wave SHM systems. They also highlight the need for compensation strategies to ensure reliable monitoring in future applications involving cryogenic hydrogen tanks, aerospace structures, and space systems.

## REFERENCES

1. S. P. E. Irving and C. Soutis, *Polymer Composites in the Aerospace Industry*, 2nd ed. Cambridge, UK: Woodhead Publishing, 2014.
2. D. A. McCarville, K. R. Meacham, J. S. McKnight, and J. M. Wood, *Design, Manufacture and Test of Cryotank Components*. Amsterdam: Elsevier, 2018.
3. C. Boller, F.-K. Chang, and Y. Fujino (Eds.), *Encyclopedia of Structural Health Monitoring*. Hoboken, NJ: John Wiley & Sons, Ltd, 2009.
4. V. Janapati, M. Seaver, S. F. Masri, F.-K. Chang, and M. J. Todd, "Damage detection sensitivity characterization of guided wave SHM," *Structural Health Monitoring*, vol. 15, no. 2, pp. 143–161, 2016.
5. R. Talreja and C. V. Singh, *Damage and Failure of Composite Materials*. Cambridge: Cambridge University Press, 2012.
6. S. Sánchez-Sáez, E. Barbero, R. Zaera, and C. Navarro, "Static behavior of CFRPs at low temperatures," *Composites Part B: Engineering*, vol. 33, no. 5, pp. 383–390, 2002.
7. S. Sánchez-Sáez, E. Barbero, R. Zaera, and C. Navarro, "Low temperature effects on CFRP mechanical properties," *Composites Part B: Engineering*, vol. 33, pp. 383–390, 2002.
8. S. Kessler, S. Spearing, and C. Soutis, "Damage detection in composite materials using Lamb wave methods," *Smart Materials and Structures*, vol. 11, no. 2, pp. 269–278, 2002.
9. B. Eckstein, D. V. Martin, and G. Gollnick, "Environmental effects on guided ultrasonic waves," in *Proc. Eur. Workshop on Structural Health Monitoring (EWSHM)*, Nantes, France, 2014.
10. M. Moix-Bonet, A. Ruiz, and J. M. Serra, "Temperature compensation for damage detection," in *Proc. Eur. Workshop on Structural Health Monitoring (EWSHM)*, Manchester, UK, 2018.
11. X. L. Zhang, R. X. Guo, and A. S. Bhalla, "Dielectric and piezoelectric properties of PZT ceramics at low temperatures," *Journal of Materials Science*, vol. 18, pp. 968–972, 1983.
12. G. H. Haertling, "Ferroelectric ceramics: History and technology," *Journal of the American Ceramic Society*, vol. 82, no. 4, pp. 797–818, 1999.
13. Qing, X.P.; Beard, S.J.; Kumar, A.; Sullivan, K.; Aguilar, R.; Merchant, M.; Taniguchi, M. The performance of a piezoelectric-sensor-based SHM system under a combined cryogenic temperature and vibration environment. *Smart Mater. Struct.* 2008, 17, 055010
14. S. Galiana, M. Moix-Bonet, D. Schmidt, and P. Wierach, "Effect of Cryogenic Temperatures on Guided Waves Structural Health Monitoring Using Acousto-Ultrasonic Piezocomposite Transducers on Composite Structures," in *Proc. Eur. Workshop on Structural Health Monitoring (EWSHM)*, Potsdam, DE, 2024